





Preparation of fabric strain sensor based on graphene for human motion monitoring

Hanna Lee¹, Mary J. Glasper², Xinda Li³, John A. Nychka³, Jane Batcheller², Hyun-Joong Chung³ , and Yi Chen^{3,4,*} 

¹Department of Chemical Engineering, McGill University, Montreal, QC H3A 0C5, Canada

²Department of Human Ecology, University of Alberta, Edmonton, AB T6G 2N1, Canada

³Department of Chemical and Materials Engineering, University of Alberta, Edmonton, AB T6G 1H9, Canada

⁴Scion, Private Bag 3020, Rotorua 3046, New Zealand

Received: 15 September 2017

Accepted: 2 March 2018

Published online:
19 March 2018

© Springer Science+Business
Media, LLC, part of Springer
Nature 2018

ABSTRACT

To date, wearable sensors are increasingly finding their way into application of healthcare monitoring, body motion detection and so forth. A stretchable and wearable strain sensor was fabricated on the basis of commercially available spandex/nylon fabric by the integration of conductive graphene network. Specifically, a simple graphene oxide dip-reduce method that enabled scalable fabrication pathway was employed. The good recovery of the graphene-coated fabric led to consistent resistance values despite the strain applied on the fabric and exhibited high gauge factor around 18.5 at 40.6% strain. Moreover, the graphene-coated fabric sensor could detect human motions such as finger bending with acceptable mechanical properties against un-coated fabrics, indicating that it has huge potential in wearable sensors applications.

Introduction

Human motion monitoring is the key element for wearable sensors for healthcare applications [1–8]. Two-dimensional (2D) conductive carbonaceous materials such as graphene and carbon nanotube embedded in elastomeric matrix have been suggested as a solution [9–12]. The degree of contact between the conductive fillers is modulated by strain exerted to the matrix material; contact between the conductors is off/on when the material is stretched/released. However, the success of wearable sensors is

heavily dependent on the comfortableness felt by the wearer; the monolithic structure of the aforementioned elastomeric composite poses a challenge in air and moisture permeability, which can cause discomfort for the wearer.

Monitoring the motion of joints, such as elbows, knees, shoulders and fingers, is subject to difficulties caused by the large amount of deformation and fast movement. The monitoring sensor must accommodate a large amount of strain, with high durability to repetitive cycles, a fast response and low creep deformation, whereas the sensor should not obstruct or interfere with the natural motion of the joint.

Address correspondence to E-mail: yi.chen@scionresearch.com

Knitted textiles are ideal vehicles for the wearable strain sensor application due to their unique fabric structure. The knitted structure intrinsically possesses pores between the yarns, which can serve as moisture-permeating and heat-insulating component. In garments, key stretch points such as the knees and elbows require up to 50% stretch [13, 14]. The desired stretch can be created by both the fibres and the fabric structure; circular weft-knit jersey fabrics provide some stretch, but the greatest stretch and recovery comes from the use of highly elastic fibres such as spandex. Spandex has been widely used in athletic wear, uniforms, swimwear and workout clothing due to its outstanding elongation and recovery properties. Spandex fibres are comprised of > 85% segmented polyurethane [15], exhibit elongations at break of 400–700% and can recover nearly completely from high elongations [15, 16]. Spandex fibres are often used with nylon fibres where stretch and recovery are needed [17]. Spandex has > 85% of its polyamide units attached directly to two aromatic rings and has “very good” elastic recovery from elongations up to 10%, with dry elongations at break from 19 to 40% [15].

Although graphene-coated fabric sensors have been attracting attention for several years, few studies have been done to investigate treatment effect (e.g. heat, chemicals and solvents) on mechanical properties (i.e. elongation and recovery changes) of fabrics, especially knitted fabrics, in order to provide a comfortable feeling for wearers [18, 19]. In this study, we introduced a scalable pathway to convert a conventional nylon/spandex knitted fabric into a stretchable and conductive strain sensor for human motion monitoring. We demonstrated the graphene-coated fabric is capable of strain sensing with high gauge factor ($GF = 18.24$ within 40.6% strain). Furthermore, the as-coated fabrics were tested to monitor human finger motion with slight and forceful bending. The effect of the graphene coating on the mechanical properties of the fabrics for potential wearable sensor applications was also discussed.

Experimental methods

Preparation of graphene-coated fabrics

A commercial weft-knit jersey fabric (90% nylon/10% spandex, 99.5 g m^{-2} , 12 wales \times 26 courses cm^{-1}) was cut into small pieces with width by length of

$5.5 \times 4.5 \text{ cm}^2$, followed by cleaning with deionized (DI) water and isopropanol, and finally dried at 90 °C for 10 min. The pre-cleaned fabrics were biaxially stretched on a grid-patterned plastic base with 20% strain for both directions. The fabric specimens were then completely submerged in a graphene oxide (GO) solution (4 mg mL^{-1} , Graphenea, Spain) for 1 min and then transferred to a convection oven at 100 °C for 90 min to dry completely. This dip-coating procedure was repeated to obtain different mass contents of GO-coated fabric specimens (1 dip, 5 dips and 10 dips). Finally, the as-coated fabric specimens were completely dried in oven.

After drying, the GO/fabrics were un-stretched and reduced to graphene/fabrics using L-ascorbic acid [20, 21]. The as-prepared GO/fabrics were placed in an 8 mg mL^{-1} L-ascorbic acid (L-AA, Sigma-Aldrich) aqueous solution and the solution was heated up to 90 °C for 24 h. The as-prepared graphene/fabrics pieces were rinsed with DI water and isopropanol and then placed in the convection oven (95 °C) to dry completely (Fig. 1).

Characterization of graphene-coated fabrics

A field emission scanning electron microscope (FE-SEM, Zeiss Sigma) was performed to obtain further morphological details of the as-coated fabrics. The resistance of obtained fabrics was measured with a digital multimeter.

The strain sensitivity of graphene/fabrics was further tested. The sample was placed between the external jaws of the caliper and held by two large metal clips which were connected to a digital source meter. The relative electrical property change was measured by the digital source meter as the strain sensor was stretched. As the fabrics were stretched according to the given strain, their respective current values were recorded. The voltage of the voltmeter was set to 1 V.

To investigate whether the dip-and-reduce procedure had detrimental effects on the mechanical properties of the fabrics, stretch and recovery tests of the treated fabrics were conducted using ASTM D2594 [22]. Eight specimens, four wale-wise (lengthwise) and four course-wise (width-wise), were cut into $5.1 \text{ cm} \times 12.7 \text{ cm}$ specimens from the untreated fabrics and the as-prepared graphene/fabrics and were conditioned as outlined in ASTM D1776 [23]. Tension was applied to each

specimen by adding weight (214 ± 0.5 g) and holding for 30 min. The fabric stretch ratio is calculated using Eq. 1.

$$\% \text{Stretch} = \frac{l_1 - l_0}{l_0} \times 100 \quad (1)$$

where l_0 is the initial length of testing specimen while l_1 is the length of testing specimen under loading.

The fabric growth ratio is also calculated using Eq. 2

$$\% \text{Growth} = \frac{l_2 - l_0}{l_0} \times 100 \quad (2)$$

where l_0 is the initial length of testing specimen while l_2 is the length of testing specimen after loading removed.

Detection of human finger motion

The graphene-coated fabric was placed vertically along a finger pointing upwards. Two of the electrical wires were then placed in contact with the fabric and taped together on the finger. These wires were connected to the digital source meter. The current measurements versus time were recorded for each motion. There were two types of motions that were performed to evaluate the sensitivity of the fabric—slight bending and the forceful bending of the finger. The bending motion was repeated every 10 s for a total of 120 s. After 60 s of slight bending, the following 60 s were carried out with forceful bending of the finger.

Results and discussion

The low- and high-magnification SEM images of the pristine fabric indicate that the diameter of nylon fibre was about $10 \mu\text{m}$ and the surface of nylon fibre was smooth, which would enhance the capillary flow of GO dispersion through the inter-fibre area during dip coating (wicking ability), resulting coating effectiveness improvement [24]. An interconnected ultra-thin GO network sheets were also observed from the SEM image of 10 dips GO/fabric composite (Fig. S1). After GO reduction, the graphene layers assembled 3D pathways on the fabrics as shown in Fig. 2b, d. The graphene layers formed a large surface not only over the fibres, but also making a contact with other layers to form a network as shown in Fig. 2d [2, 3], which significantly enhance the conductivity of as-coated fabrics. Furthermore, it was clearly shown that the wrinkles around the individual fibres (Fig. 2b) were attributed to the different thermal expansions of graphene [21, 25]. Furthermore, there was no obvious change in reduced GO thickness with different GO dipping cycles, but the interconnection between individual fabrics increased by graphene bridging, which elevated the conductivity (Fig. S2).

Figure 3 depicts the relationship between the resistance of graphene/fabrics and GO deposition cycles. As the number of dips increased, the connectivity between graphene-coated area improved and their thickness increased. Consequently, the resistance of the graphene-coated fabrics decreased from 1.37 ± 0.84 to 0.22 ± 0.02 k Ω with the increase in dipping steps. The mean standard deviation (SD) of the resistance of coated fabrics also decreased and

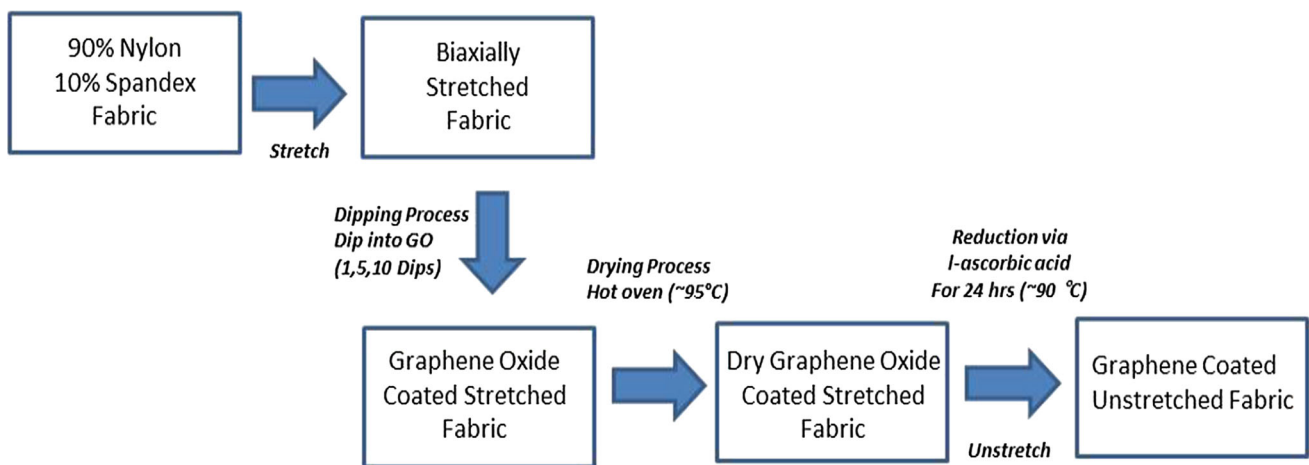


Figure 1 Schematics of the fabrication procedure of the graphene/fabrics.

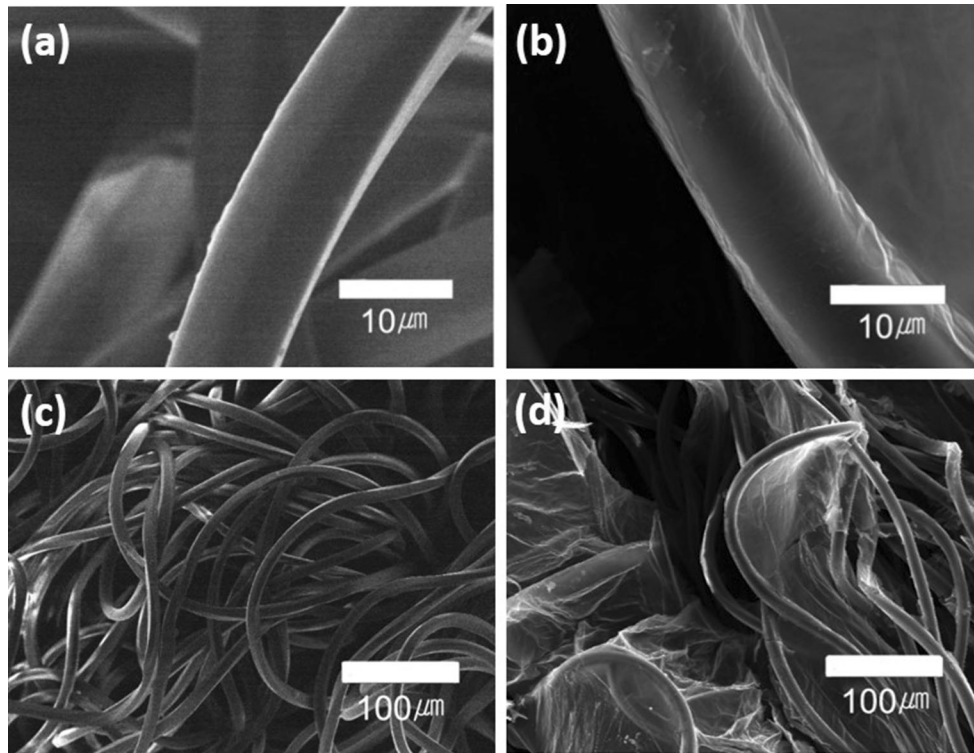


Figure 2 SEM images of the fabric that went through a, c no treatment and b, d 10 time deposition cycles.

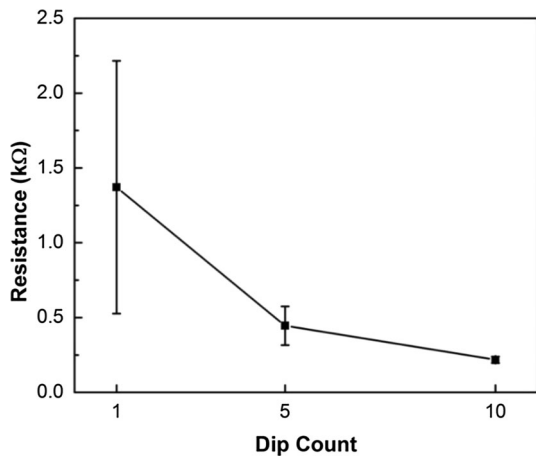


Figure 3 Resistance of the graphene-coated fabrics prepared with 1, 5 and 10 dips.

provided a high uniform sheet resistance over large area. Between 1 dip and 5 dips, drastic decreases in resistance values and their standard deviation were observed, but the further difference observed between 5 and 10 dips was not as dramatic as the first 1 dip and 5 dips. This indicates that percolation between electrically conducting graphene-coated regions was achieved within the first 5 dips.

To investigate the strain sensing performance, the current change of graphene/fabrics was traced under various strain loading condition. Figure 4 demonstrates a pattern that the fabrics were stretched up to 0, 6.67, 13.3, 20.0, 26.7, 33.3 and 40.0%. The 10 dips sample was chosen as the testing samples in this study. Grey shadows represent the transition stage

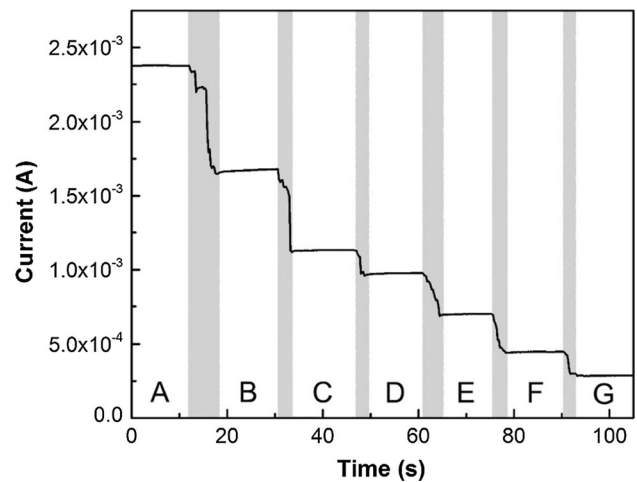


Figure 4 Relative current change of 10 dips sample over time for strain of A = 0%, B = 6.67%, C = 13.3%, D = 20.0%, E = 26.7%, F = 33.3% and G = 40.0%.

where the fabric was in a process of stretching and therefore can be ignored. The decrease in electrical current values was due to an increasing distance between graphene layers when the strain was applied [7, 26–28]. When the distance between graphene layers increases, it caused the overlapping area between adjacent graphene layers to decrease, hence the graphene layers that were acting as a bridge for the current to flow disconnect.

The relative resistance change of 10 dips samples was further characterized versus the applied strain (%) to evaluate the sensitivity of the strain sensor. Figure 5 illustrates the resistance variation ($\Delta R/R_0$) of 10 dips graphene/fabrics under tensile strain. The slope of the resistance versus strain also increased, respectively. The gauge factor (GF), which is the representative parameter to evaluate the sensitivity of the strain sensor, was evaluated by $(\Delta R/R_0)/\varepsilon$, where ε is the strain [1, 9]. The GF of the coated fabric was 6.33 within 6.67% strain and 18.24 within 40.6% strain. The relatively higher GF was superior or comparable to most of the previously published graphene-based strain sensor [7, 26–29], which endowed the fabric-based sensor with a controllable combination of high sensitivity at small strain and broad sensing range.

We further investigated the behaviours of the strain sensor for human motion monitoring. The fabric strain sensor was attached onto a glove to detect the change of figure bending (Fig. 6a). When

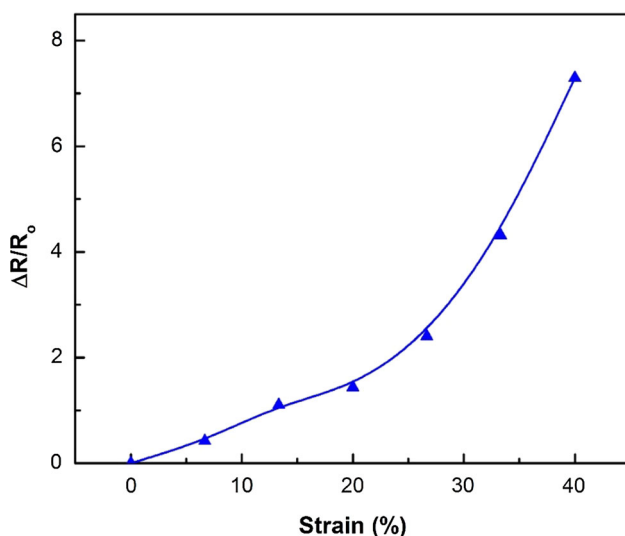


Figure 5 Relative resistance change of the 10 dips of graphene-coated fabric as a function of applied strain.

the fabric was bent slightly, the relative resistance change values stayed over 280% with rapid response. Although the sensitivity fluctuated slightly while the bending motion was forceful, they remained relatively consistent throughout the tests within the range between 460 and 540% (Fig. 6b). The high sensitivity and good repeatability of these measurements show that the graphene-coated fabrics were able to monitor different parts of the human body motions. It can be also noticed that this sensor was very flexible which would enable to integrate with textile-based wearable devices, so as to monitor body motion. However, more experiments need to be conducted to evaluate the long-term stability of the fabric as a sensor.

Mechanical properties such as elongation and recovery in both wale and course direction are the most critical factors for knit fabrics in terms of giving excellent comfortable feeling to wearers. A knitted structure of fabric is shown in Fig. 7a, b, indicating both wale and course of knit structure. Figure 7c and d shows the elongation of the untreated fabric samples had a maximum elongation of 253% in the wales direction, and 267% in the courses direction. Weft-knitted fabrics often exhibit anisotropic deformation with the course direction typically having substantially higher stretch than the wale direction. It was due to increased yarn slippage within the fabric structure to accommodate the strain [30]. The high percentage of spandex in this fabric likely increased the amount of stretch in the wale direction beyond what would be expected without the spandex, enabling greater extension in the yarn stretch step of the weft-knit deformation [30]. The elongation and recovery of pure water and L-AA treated samples showed less changes in both wale and course direction compared with untreated samples (Fig. S4). The graphene-treated fabrics showed a marked decrease in elongation compared to the samples without graphene saturation, and the maximum elongation of the graphene-treated fabrics was 124 and 121% in the wale and course directions, respectively.

The different amount of stretch seen in the graphene-treated fabrics can be attributed to several different factors; one being the graphene physically interfering with the fabric's ability to stretch. The graphene could be preventing the yarns from sliding past each other to accommodate the strain, due to its high tensile strength. Graphene is known for

Figure 6 **a** Photography of the fabric-based sensor attached onto the finger for analysis of the bending motion, **b** relative resistance change over time according to the motion of the finger.

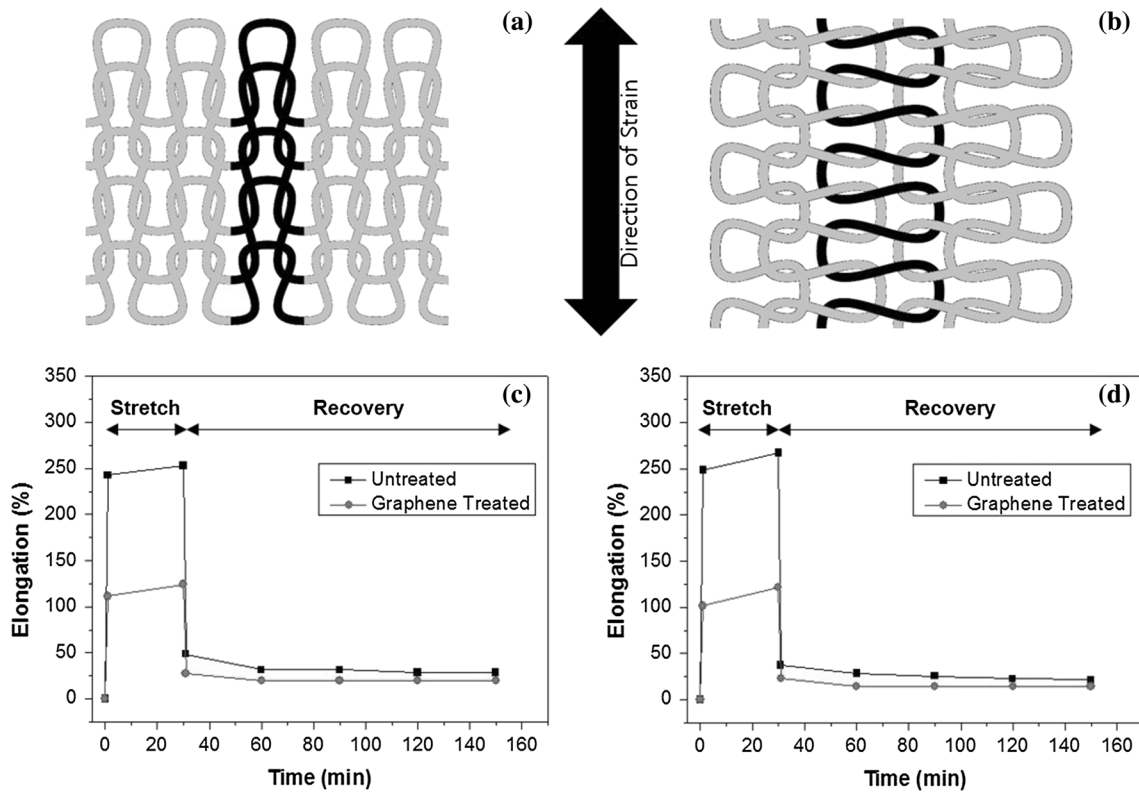
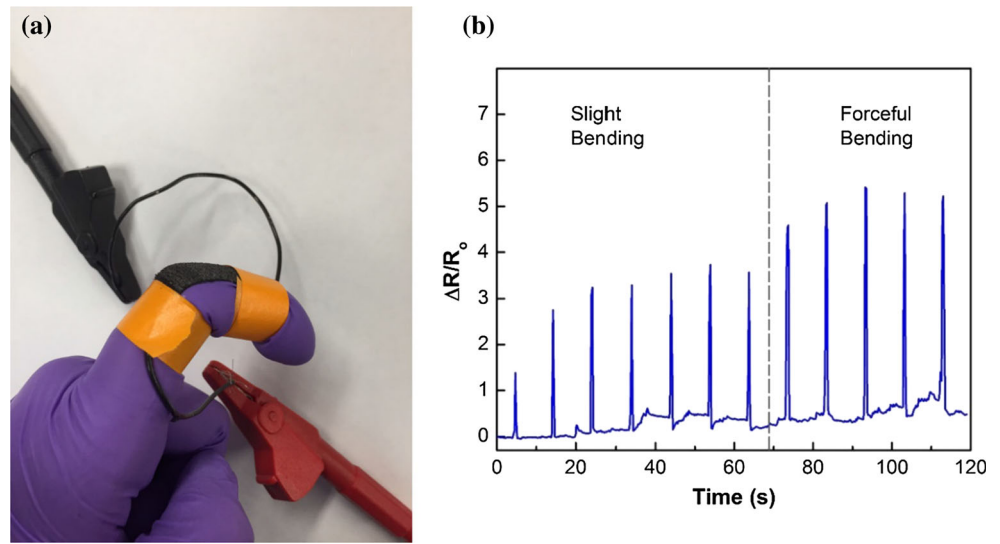


Figure 7 Schematic description of the fabric pattern of **a** wale-wise and **b** course-wise. Stretch and recovery performance of fabrics in wale direction **a** and course direction **b**.

its strong intrinsic material properties, including a very high ultimate tensile strength of 130 GPa [31]. Moreover, the presence of graphene wrinkles may change the texture of the fabric surface into more rough and unrefined [32]. Due to this physical

interference, the fabrics treated with graphene exhibited substantially less extension than the other fabrics, and as a result, mostly recovered to their original length (20 and 14% growth ratio in the wale and course directions, respectively).

From the stretch and recovery experiment, it was apparent that although the fabrics lose most of their ability to stretch after being treated with graphene, the recovery stage shows high recovery rate, with the values staying steady. More importantly, the graphene-treated fabrics stretched beyond the required 50% for key stretch points and recovered with a minimal amount of growth, which would enable proper fit. Therefore, this fabrics based strain sensor as a wearable device has great potential in the detection of human body and health.

Conclusions

A stretchable and wearable graphene/fabric strain sensor has been fabricated by a simple and scalable dipping-reduce method with commercial spandex/nylon fabrics as a starting material. The strain sensor showed good conductivity and high GF of 18.24 within 40.6% strain, which could be ascribed to the highly conductive graphene network and good elongation and recovery properties of spandex/nylon fabric. It was demonstrated successfully that the resulting strain sensor was able to monitor human body motion such as finger bending. The further results showed that although the stretch and recovery changes of the graphene-treated fabrics were decreased in both wale and course direction and became less pliable, it could provide a comfortable feeling for wearers, indicating this strain sensor could be adapted for wearable human motion sensing. In addition to high GF and good mechanical properties, the performance repeatability of the fabric strain sensor is also important; the repeatability will be evaluated in the future.

Acknowledgements

We acknowledge the NSERC RGPIN 435914 for financial support of this work.

Authors contribution HL, MG, HC and YC conceived ideas. HL, MG and XL performed experiments. XL and HC established graphene reduction protocols. HL and MG wrote manuscript. All authors have given approval to the final version of the manuscript.

Compliance with ethical standards

Conflict of interest The authors declare that there is no conflict of interest regarding the publication of this paper.

Electronic supplementary material: The online version of this article (<https://doi.org/10.1007/s10853-018-2194-7>) contains supplementary material, which is available to authorized users.

References

- [1] Trung TQ, Lee N-E (2016) Flexible and stretchable physical sensor integrated platforms for wearable human-activity monitoring and personal healthcare. *Adv Mater* 28(22):4338–4372. <https://doi.org/10.1002/adma.201504244>
- [2] Kang HG, Mahoney DF, Hoenig H, Hirth VA, Bonato P, Hajjar I, Lipsitz LA (2010) In situ monitoring of health in older adults: technologies and issues. *J Am Geriatr Soc* 58(8):1579–1586
- [3] Paradiso R, Loriga G, Taccini N (2004) Wearable system for vital signs monitoring. *Stud Health Technol Inform* 108:253–259
- [4] Teng X-F, Zhang Y-T, Poon CCY, Bonato P (2008) Wearable medical systems for p-Health. *IEEE Rev Biomed Eng* 1:62–74
- [5] Webb RC, Bonifas AP, Behnaz A, Zhang Y, Yu KJ, Cheng H, Shi M, Bian Z, Liu Z, Kim YS, Yeo WH, Park JS, Song J, Li Y, Huang Y, Gorbach AM, Rongers JA (2013) Ultrathin conformal devices for precise and continuous thermal characterization of human skin. *Nat Mater* 12(10):938–944. <https://doi.org/10.1038/nmat3755>
- [6] Amjadi M, Kyung K-U, Park I, Sitti M (2016) Stretchable, skin-mountable, and wearable strain sensors and their potential applications: a review. *Adv Funct Mater* 26(11):1678–1698. <https://doi.org/10.1002/adfm.201504755>
- [7] Wang Y, Wang L, Yang T, Li X, Zang X, Zhu M, Wang K, Wu D, Zhu H (2014) Wearable and highly sensitive graphene strain sensors for human motion monitoring. *Adv Funct Mater* 24(29):4666–4670. <https://doi.org/10.1002/adfm.201400379>
- [8] Yeo WH, Kim YS, Lee J, Ameen A, Shi L, Li M, Wang S, Ma R, Jin SH, Kang Z, Rongers JA (2013) Multifunctional epidermal electronics printed directly onto the skin. *Adv Mater* 25(20):2773–2778. <https://doi.org/10.1002/adma.201204426>

- [9] Amjadi M, Pichitpajongkit A, Lee S, Ryu S, Park I (2014) Highly stretchable and sensitive strain sensor based on silver nanowire-elastomer nanocomposite. *ACS Nano* 8(5):5154–5163. <https://doi.org/10.1021/nn501204t>
- [10] Choong C-L, Shim M-B, Lee B-S, Jeon S, Ko D-S, Kang T-H, Bae J, Lee SH, Bryun K-E, Im J, Jeong YJ, Park C, Park J-J, Chung U-I (2014) Highly stretchable resistive pressure sensors using a conductive elastomeric composite on a micropillar array. *Adv Mater* 26(21):3451–3458. <https://doi.org/10.1002/adma.201305182>
- [11] Muth JT, Vogt DM, Truby RL, Kolesky DB, Wood RJ, Lewis JA et al (2014) Menguc Y. *Adv Mater* 26(36):6307–6312. <https://doi.org/10.1002/adma.201400334>
- [12] Shin MK, Oh J, Lima M, Kozlov ME, Kim SJ, Baughman RH (2010) Elastomeric conductive composites based on carbon nanotube forests. *Adv Mater* 22(24):2663–2667. <https://doi.org/10.1002/adma.200904270>
- [13] Voyce J, Dafniotis P, Towilson S (2005) *Textiles in sport*. Woodhead Publishing, UK
- [14] Chattopadhyay R, Gupta D, Bera M (2012) Effect of input tension of inlay yarn on the characteristics of knitted circular stretch fabrics and pressure generation. *J Text I* 103:636–642. <https://doi.org/10.1080/00405000.2012.665237>
- [15] Needles HL (1981) *Handbook of textile fibers, dyes, and finishes*. Garland STPM Press, New York
- [16] Hepburn C (1982) *Polyurethane elastomers*. Applied Science Publishers, UK
- [17] Hughes AJ, McIntyre JE, Clayton G, Wright P, Poynton DJ, Atkinson J, Morgan PE, Rose L, Stevenson PA, Mohajer AA, Ferguson WJ (1976) The production of man-made fibres. *Text Prog* 8(1):1–156. <https://doi.org/10.1080/00405167608688984>
- [18] Maziz A, Concas A, Khaldi A, Stålhund J, Persson N-K, Jager EWH (2017) Knitting and weaving artificial muscles. *Sci Adv* 3:e1600327. <https://doi.org/10.1126/sciadv.1600327>
- [19] Atalay O, Kennon W, Husain M (2013) Textile-based weft knitted strain sensors: effect of fabric parameters on sensor properties. *Sensors* 13(8):11114–11127. <https://doi.org/10.3390/s130811114>
- [20] Zhang J, Yang H, Shen G, Cheng P, Zhang J, Guo S (2010) Reduction of graphene oxide vial-ascorbic acid. *Chem Commun* 46:1112–1114. <https://doi.org/10.1039/B917705A>
- [21] Li X, Chen Y, Kumar A, Mahmoud A, Nychka JA, Chung H-J (2015) Sponge-templated macroporous graphene network for piezoelectric ZnO nanogenerator. *ACS Appl Mater Interfaces* 7(37):20753–20760. <https://doi.org/10.1021/acsami.5b05702>
- [22] ASTM D2594-04 (2004) Standard test method for stretch properties of knitted fabrics having low power. ASTM International, West Conshohocken
- [23] ASTM D1776-04 (2004) Standard practice for conditioning and testing textiles. ASTM International, West Conshohocken
- [24] Patnaik A, Rengasamy RS, Kothari VK, Ghosh A (2006) Wetting and wicking in fibrous materials. *Text Prog* 38:1–105. <https://doi.org/10.1533/jotp.2006.38.1.1>
- [25] Yun YJ, Hong WG, Kim W-J, Jun Y, Kim BH (2013) A novel method for applying reduced graphene oxide directly to electronic textiles from yarns to fabrics. *Adv Mater* 25(40):5701–5705. <https://doi.org/10.1002/adma.201303225>
- [26] Chen S, Wei Y, Yuan X, Lin Y, Liu L (2016) A highly stretchable strain sensor based on a graphene/silver nanoparticle synergic conductive network and a sandwich structure. *J Mater Chem C* 4:4304–4311. <https://doi.org/10.1039/C6TC00300A>
- [27] Yan C, Wang J, Kang W, Cui M, Wang X, Foo CY, Chee KJ, Lee PS (2014) Highly stretchable piezoresistive graphene-nanocellulose nanopaper for strain sensors. *Adv Mater* 26(13):2022–2027. <https://doi.org/10.1002/adma.201304742>
- [28] Tian H, Shu Y, Cui Y-L, Mi W-T, Yang Y, Xie D, Ren T-L (2014) Scalable fabrication of high-performance and flexible graphene strain sensors. *Nanoscale* 6:699–705. <https://doi.org/10.1039/C3NR04521H>
- [29] Cai G, Yang M, Xu Z, Liu J, Tang B, Wang X (2017) Flexible and wearable strain sensing fabrics. *Chem Eng J* 325:396–403. <https://doi.org/10.1016/j.cej.2017.05.091>
- [30] Wang J, Xue P, Tao X, Yu T (2014) Strain sensing behavior and its mechanisms of electrically conductive PPy-coated fabric. *Adv Eng Mater* 16(5):565–570. <https://doi.org/10.1002/adem.201300407>
- [31] Lee C, Wei X, Kysar JW, Hone J (2008) Measurement of the elastic properties and intrinsic strength of monolayer graphene. *Science* 321(5887):385–388
- [32] Ramanathan T, Abdala AA, Stankovich S, Dikin DA, Herrera-Alonso M, Piner RD, Adamson DH, Schniepp HC, Chen X, Ruff RS, Nguyen ST, Aksay IA, Prud'Homme RK, Brinson LC (2008) Functionalized graphene sheets for polymer nanocomposites. *Nat Nano* 3:327–331. <https://doi.org/10.1038/nnano.2008.96>